Contrasting Pathways for the Reactions of Triruthenaborane Cluster Anions with $[\{M(\eta^5\text{-}C_5Me_5)Cl_2\}_2]$(M = Rh or Ir). Molecular Structures of $[RhRu_3(\eta^5\text{-}C_5Me_5)H_2(CO)_8(PPh_3)BH]$ and $[IrRu_3(\eta^5\text{-}C_5Me_5)H(CO)_{10}BH_2]$‡

Jane R. Galsworthy,[a] **Catherine E. Housecroft,***†[a] **Dorn M. Matthews,**[a] **Robert Ostrander**[b] **and Arnold L. Rheingold***[b]

[a] *University Chemical Laboratory, Lensfield Road, Cambridge CB2 1EW, UK*

[b] *Department of Chemistry, University of Delaware, Newark, DE 19716, USA*

The reactions of $[N(PPh_3)_2][Ru_3(CO)_9BH_4]$ and $[N(PPh_3)_2][Ru_3(CO)_9(B_2H_5)]$ with $[\{M(\eta^5\text{-}C_5Me_5)Cl_2\}_2]$ (M = Rh or Ir) follow two different, but related, pathways. For M = Rh, the products in each case are the 62-electron butterfly borido-cluster $[RhRu_3(\eta^5\text{-}C_5Me_5)H(CO)_9BH_2]$ **1** and the tetrahedral cluster $[RhRu_3(\eta^5\text{-}C_5Me_5)H_2(CO)_{10}]$. In contrast, the reaction of $[\{Ir(\eta^5\text{-}C_5Me_5)Cl_2\}_2]$ with $[N(PPh_3)_2][Ru_3(CO)_9BH_4]$ leads to the 64-electron cluster $[IrRu_3(\eta^5\text{-}C_5Me_5)H(CO)_{10}BH_2]$ **4** and tetrahedral $[IrRu_3(\eta^5\text{-}C_5Me_5)H_4(CO)_9]$ **3** but when the starting cluster is $[Ru_3(CO)_9(B_2H_5)]^-$, only **4** is formed. A single-crystal X-ray diffraction analysis of compound **4** has been carried out: triclinic, space group $P\bar{1}$, $a = 8.780(1)$, $b = 12.304(3)$, $c = 12.432(3)$ Å, $\alpha = 105.78(2)$, $\beta = 93.55(2)$, $\gamma = 91.44(2)°$, $Z = 2$, $R = 0.0483$. The Ru_3Ir cluster core in **4** can be described either as an open-butterfly or a spiked triangle which is supported by a μ_4-boron atom [Ir–B 2.04(1) Å and Ru–B(av.) 2.28(1) Å]. In solution, two isomers of $[IrRu_3(\eta^5\text{-}C_5Me_5)H(CO)_{10}BH_2]$, which differ in the positions of cluster hydrogen atoms, are observed. Compound **1** reacts with PPh_3 to give $[RhRu_3(\eta^5\text{-}C_5Me_5)H_2(CO)_8(PPh_3)BH]$ **5**. The crystal structure of compound **5** has been determined and the results confirm the presence of a heterometallic butterfly core: monoclinic, space group $P2_1/n$, $a = 11.538(1)$, $b = 18.141(2)$, $c = 19.089(3)$ Å, $\beta = 102.98(1)°$, $Z = 4$, $R = 0.0368$. A comparison of the ^{11}B and ^1H NMR spectroscopic data for **1** and **5** indicates that a redistribution of cluster hydrogen atoms occurs during the substitution of a phosphine for carbonyl ligand; one Ru–H–B and two Ru–H–Ru bridging hydrogen atoms have been located directly in **5** by X-ray diffraction.

Butterfly boride clusters of general formula $[M_4H(CO)_{12}BH_2]$ where M is iron,[1,2] ruthenium[3,4] or osmium[5] have been prepared and fully characterised. We have shown that a heterometal atom can be introduced into the wing-tip site of the ruthenium butterfly to give compounds of the type $[FeRu_3H(CO)_{12}BH_2]$,[6] $[MoRu_3(cp)H(CO)_{11}BH]$,[7] $[WRu_3(cp)H(CO)_{11}BH]$ (cp = $\eta^5\text{-}C_5H_5$).[7] Suitable precursors to these heterometallic boride clusters are the triruthenaborane clusters $[Ru_3(CO)_9(B_2H_6)]$,[7] $[Ru_3(CO)_9BH_5]$[6,7] and its conjugate base, $[Ru_3(CO)_9BH_4]^-$.[6] The strategy for constructing heterometal $M'M_3E$ cages by adding an M′-containing fragment to a tetrahedral core of type M_3E has also been illustrated for E = C[8-12] and O.[13] The introduction of a heterometal, M′, into an M_4B cage to give new clusters with cores of type $M'_xM_{4-x}B$ should perturb the electronic structure of the metal cage around the semi-interstitial boron atom and hence alter the reactivity of that atom. Changes in electronic structure of heterometal carbide clusters, (containing an $M'M_3C$ core), with respect to homometallic analogues are supported by theoretical studies.[8]

In our investigations of the use of $[Ru_3(CO)_9BH_4]^-$ and $[Ru_3(CO)_9(B_2H_5)]^-$ as precursors to higher nuclearity boron-containing clusters, we have found that the products of the reactions with $[\{M(\eta^5\text{-}C_5Me_5)Cl_2\}_2]$ (M = Rh or Ir) are dependent upon M; the reactions yield a closed- or an unexpected, open-butterfly cluster for M = Rh or Ir, respectively, and we herein report our new results.

Experimental

General.—Fourier-transform NMR spectra were recorded on a Bruker WM 250 or AM 400 spectrometer. Proton NMR shifts are reported with respect to δ 0 for $SiMe_4$; ^{11}B NMR with respect to δ 0 for $BF_3\cdot OEt_2$; ^{31}P NMR with respect to δ 0 H_3PO_4. All downfield chemical shifts are positive. Infrared spectra were recorded on a Perkin-Elmer FT 1710 spectrophotometer. Fast atom bombardment (FAB) mass spectra were recorded on Kratos instruments using 3-nitrobenzyl alcohol as the matrix.

All reactions were carried out under argon by using standard Schlenk techniques. Solvents were dried over suitable reagents and freshly distilled under N_2 before use. Separations were carried out by thin-layer plate chromatography with Kieselgel 60-PF-254 (Merck). The dimers $[\{M(\eta^5\text{-}C_5Me_5)Cl_2\}_2]$ (M = Rh or Ir) were used as received (Aldrich). The compounds $[N(PPh_3)_2][Ru_3(CO)_9BH_4]$[6] and $[N(PPh_3)_2][Ru_3(CO)_9(B_2H_5)]$[14] were prepared as previously described. Yields given are those obtained for a typical reaction, based on the Ru_3-starting cluster.

Reactions.—$[N(PPh_3)_2][Ru_3(CO)_9BH_4]$ *with* $[\{Rh(\eta^5\text{-}C_5Me_5)Cl_2\}_2]$. The compound $[\{Rh(\eta^5\text{-}C_5Me_5)Cl_2\}_2]$ (62 mg, 0.1 mmol) was dissolved in CH_2Cl_2 (10 cm^3) and was added to a solution of $[N(PPh_3)_2][Ru_3(CO)_9BH_4]$ (111 mg, 0.1 mmol) in CH_2Cl_2 (10 cm^3). A colour change from yellow to red was immediately observed. After stirring the solution for 1 h, the solvent was removed *in vacuo* and the products were separated

---

† *Present address:* Institut für Anorganische Chemie, Spitalstrasse 51, CH-4056 Basel, Switzerland.

‡ *Supplementary data available:* see Instructions for Authors, *J. Chem. Soc., Dalton Trans.*, 1994, Issue 1, pp. xxiii–xxviii.

by TLC, eluting with hexane. Initial, yellow, fractions included $[Ru_3(CO)_9BH_5]$,[15] $[Ru_3(CO)_9(B_2H_6)]$[7] and $[Ru_4H(CO)_{12}BH_2]$.[3,4] The major product, collected as the fifth fraction (red) in ≈80% yield, was $[RhRu_3(\eta^5\text{-}C_5Me_5)H(CO)_9BH_2]$ **1**. The sixth fraction (brown) was identified as $[RhRu_3(\eta^5\text{-}C_5Me_5)H_2(CO)_{10}]$[16,17] but this product was only formed in small quantities (< 5%). The seventh (purple-red) fraction (< 5%) is proposed as $[RhRu_4(\eta^5\text{-}C_5Me_5)H(CO)_{12}BH_2]$ **2**. Compound **1**. NMR ($CDCl_3$, 298 K): ^1H (400 MHz), δ 2.07 (s, Me), −9.6 (vbr, $w_{\frac{1}{2}}$ = 300 Hz, B–H–Rh and B–H–Ru) and −20.29 (s, Ru–H–Ru); ^{11}B (128 MHz), δ +94.0. IR (CH_2Cl_2, cm^{-1}) ν_{CO} 2075m, 2037vs, 2006m, 1982m and 1942vw. FAB mass spectrum: *m/z* 807 (P^+) (calc. for $^{12}C_{19}{}^1H_{18}{}^{11}B_1{}^{16}O_9{}^{103}Rh_1{}^{101}Ru_3$ 807) with seven CO losses. Compound **2**. NMR ($CDCl_3$, 298 K): ^1H, δ 1.98 (s, Me), −8.9 (br, B–H–Ru or B–H–Rh, see text), −10.2 (br, B–H–Ru or B–H–Rh, see text), −20.58 (s, Ru–H–Ru); ^{11}B (128 MHz), δ +101.6 (t, J_{BH} = 75 Hz). IR (CH_2Cl_2, cm^{-1}) ν_{CO} 2088w, 2074m, 2052vs, 2026m, 2010m(sh), 1980w and 1825w. FAB mass spectrum: *m/z* 992 (P^+) (calc. for $^{12}C_{22}{}^1H_{18}{}^{11}B_1{}^{16}O_{12}{}^{103}Rh_1{}^{101}Ru_4$ 992) with seven CO losses.

$[N(PPh_3)_2][Ru_3(CO)_9(B_2H_5)]$ *with* $[\{Rh(\eta^5\text{-}C_5Me_5)Cl_2\}_2]$. The compound $[\{Rh(\eta^5\text{-}C_5Me_5)Cl_2\}_2]$ (62 mg, 0.1 mmol) was dissolved in CH_2Cl_2 (10 cm^3) and added to a solution of $[N(PPh_3)_2][Ru_3(CO)_9(B_2H_5)]$ (112 mg, 0.1 mmol) in CH_2Cl_2 (10 cm^3). The solution was stirred for 1 h, and then solvent was removed *in vacuo*. The products were separated by TLC, eluting with hexane. Approximately half of the starting cluster remained in its protonation form and was collected as the first (yellow) fraction. The second fraction (red) was **1** (≈40%). The third fraction was $[RhRu_3(\eta^5\text{-}C_5Me_5)H_2(CO)_{10}]$[16,17] but this product was formed in low yield, typically < 5%. Compound **2** was collected as the fourth fraction (< 5%).

$[N(PPh_3)_2][Ru_3(CO)_9BH_4]$ *with* $[\{Ir(\eta^5\text{-}C_5Me_5)Cl_2\}_2]$. The compound $[\{Ir(\eta^5\text{-}C_5Me_5)Cl_2\}_2]$ (77 mg, 0.1 mmol) was dissolved in CH_2Cl_2 (10 cm^3) and the solution was added to $[N(PPh_3)_2][Ru_3(CO)_9BH_4]$ (111 mg, 0.1 mmol), previously dissolved in CH_2Cl_2 (10 cm^3). The resulting solution was stirred for 1 h; the final solution was red-brown. After solvent had been removed *in vacuo*, the products were separated by TLC, eluting with hexane. Five fractions were collected. The first three fractions were identified as $[Ru_3(CO)_9BH_5]$,[14] $[Ru_3(CO)_9(B_2H_6)]$,[7] and $[Ru_4H(CO)_{12}BH_2]$,[3,4] respectively. $[IrRu_3(\eta^5\text{-}C_5Me_5)H_4(CO)_9]$ **3** was eluted as the fourth (orange, ≈5% yield) band and $[IrRu_3(\eta^5\text{-}C_5Me_5)H(CO)_{10}BH_2]$ **4** was collected as the fifth (yellow, ≈15% yield) fraction. A lower, orange fraction was discarded. The yield of **4** can be improved (up to 40%) by passing a steady stream of CO through the reaction mixture for 1 h. Compound **3**. ^1H NMR ($CDCl_3$, 298 K, 400 MHz), δ +2.20 (s, 15 H, Me) and −18.71 (s, 4 H, M–H–Ru, M = Ir or Ru, see text). IR (CH_2Cl_2, cm^{-1}) ν_{CO} 2075m, 2044vs, 2020s, 1997m, 1940w. FAB mass spectrum: *m/z* 888 (P^+) (calc. for $^{12}C_{19}{}^1H_{19}{}^{192}Ir_1{}^{16}O_9{}^{101}Ru_3$ 886) with four CO losses. Compound **4** (two isomers, see text): NMR: ^1H (CD_2Cl_2, 180 K, 400 MHz), δ 1.97 (s, Me), 1.94 (s, Me), (integrals for Me signals ≈1 : 1), −6.0 (br, B–H–Ru), −6.4 (br, B–H–Ru), −6.9 (br, B–H–Ru), −7.2 (br, B–H–Ru), −17.95 (s, Ru–H–Ru) and −18.64 (s, Ru–H–Ru), (integrals for hydride signals = 1.0 : 1.2); ^{11}B ($CDCl_3$, 298 K, 128 MHz), δ +92.7 and +89.7 (integrals ≈ 1 : 1). IR (hexane, cm^{-1}) ν_{CO} 2091vs, 2057m(sh), 2054vs, 2040m(sh), 2036s, 2026m, 2012w, 2004w, 1997vw, 1991w and 1971w. FAB mass spectrum *m/z* 926 (P^+) (calc. for $^{12}C_{20}{}^1H_{18}{}^{11}B_1{}^{192}Ir_1{}^{16}O_{10}{}^{101}Ru_3$ 924) with nine CO losses.

$[N(PPh_3)_2][Ru_3(CO)_9(B_2H_5)]$ *with* $[\{Ir(\eta^5\text{-}C_5Me_5)Cl_2\}_2]$. The compound $[N(PPh_3)_2][Ru_3(CO)_9(B_2H_5)]$ (101 mg, 0.09 mmol) and $[\{Ir(\eta^5\text{-}C_5Me_5)Cl_2\}_2]$ (69 mg, 0.09 mmol) were dissolved in CH_2Cl_2 (10 cm^3) and the solution was stirred for 1 h. After solvent had been removed *in vacuo*, the products were separated by TLC, eluting with hexane and CH_2Cl_2 (2 : 1). The first fraction to be collected consisted of $[Ru_3(CO)_9(B_2H_6)]$,[7] $[Ru_4H(CO)_{12}BH_2]$[3,4] and $[Ru_4H_4(CO)_{12}]$.[18] The second fraction was reseparated by TLC, eluting with hexane, to give one major, yellow fraction (≈10%) identified as **4**.

$[RhRu_3(\eta^5\text{-}C_5Me_5)H_2(CO)_8(PPh_3)BH]$ **5** Compound **1** (60 mg, 0.07 mmol) and PPh_3 (52 mg, 0.2 mmol) were dissolved in CH_2Cl_2 (10 cm^3). The solution was stirred at room temperature for 1 h, during which time the colour changed from red to brown. The solvent was removed *in vacuo* and the products were separated by TLC, eluting with CH_2Cl_2–hexane (1:2). $[RhRu_3(\eta^5\text{-}C_5Me_5)H_2(CO)_8(PPh_3)BH]$ **5** was collected as the second fraction (brown) almost quantitatively. NMR ($CDCl_3$): ^1H (293 K, 400 MHz), δ 1.98 (s, Me), −4.9 (br, B–H–Ru), −14.41 (d, J_{PH} = 14 Hz, Ru–H–Ru) and −20.55 (s, Ru–H–Ru); ^{11}B (298 K, 128 MHz), δ +149 (poorly resolved d, J_{BH} ≈ 35 Hz); ^{31}P (298 K, 162 MHz), δ +35.5; IR (CH_2Cl_2, cm^{-1}) ν_{CO} 2055s, 2022vs, 1995s, 1968m and 1789w. FAB mass spectrum: *m/z* 1041 (P^+) (calc. for $^{12}C_{36}{}^1H_{33}{}^{11}B_1{}^{16}O_8{}^{31}P_1{}^{103}Rh_1{}^{101}Ru_3$ 1041) with six CO losses.

Crystal Structural Determinations.—Crystallographic data for compounds **4** and **5** are given in Table 1. Both **4** and **5** were mounted on glass fibres and structures were obtained at ambient temperatures. Photographic evidence revealed $\bar{1}$ and $2/m$ Laue symmetry, respectively. For **4**, the centrosymmetric choice of space groups was initially assumed and later supported by the results of refinement; for **5**, the space group was uniquely determined by systematic absences. Both data sets were corrected for absorption by semi-empirical methods. The metal atom locations were obtained by direct methods, and the structures completed by Fourier-difference syntheses. All non-hydrogen atoms were refined with anisotropic thermal parameters. For **4**, methyl-group hydrogen atoms were idealised and the remainder, which could not be reliably located, were ignored. For **5**, methyl-group hydrogen atoms were also idealised, but the cluster-bridging hydrogen atoms were found and refined.

All computations used the SHELXTL PLUS V4.2 software.[19] Atomic coordinates for **4** and **5** are given in Tables 2 and 3, respectively.

Additional material available from the Cambridge Crystallographic Data Centre comprises H-atom coordinates, thermal parameters and remaining bond lengths and angles.

Results and Discussion

We have previously reported[7] that the reactions of $[Ru_3(CO)_9BH_5]$ and $[Ru_3(CO)_9(B_2H_6)]$ with $[\{M(cp)(CO)_3\}_2]$ (M = Mo or W) under photolytic conditions lead to $[MRu_3(cp)H(CO)_{11}BH]$ (M = Mo or W), $[MRu_3(cp)H_3(CO)_{11}]$ (M = Mo or W) and $[M_2Ru_3(cp)_2(CO)_{13}]$ (M = W). In these reactions, the $\{M(cp)(CO)_2\}$ fragment either adds to the cluster core or substitutes for an isolobal $\{BH_2\}$ unit. In an extension of our preparative and reactivity studies of heterometallic boron-containing clusters, we turned to the dimers $[\{M(\eta^5\text{-}C_5Me_5)Cl_2\}_2]$ (M = Rh or Ir) as the source of the heterometal atom. Each dimer is formally a source of the fragment $\{M(\eta^5\text{-}C_5Me_5)\}^{2+}$.

Reactions of Triruthenaborane Anions with $[\{Rh(\eta^5\text{-}C_5Me_5)Cl_2\}_2]$.—The reaction of either $[Ru_3(CO)_9BH_4]^-$ or $[Ru_3(CO)_9(B_2H_5)]^-$ with $[\{Rh(\eta^5\text{-}C_5Me_5)Cl_2\}_2]$ leads to the metallaborane clusters $[RhRu_3(\eta^5\text{-}C_5Me_5)H(CO)_9BH_2]$ **1** and $[RhRu_4(\eta^5\text{-}C_5Me_5)H(CO)_{12}BH_2]$ **2** and the non-boron containing compound $[RhRu_3(\eta^5\text{-}C_5Me_5)H_2(CO)_{10}]$.[16,17] Thus, the reaction pathway appears to be quite similar to those reported by us for incorporation of molybdenum and tungsten fragments.[7]

Cluster **1** is isoelectronic with $[Ru_4H(CO)_{12}BH_2]$ and similarities in the NMR spectroscopic properties of the two clusters support similarities in structure. The ^{11}B NMR spectrum of **1** exhibits an unresolved signal ($w_{\frac{1}{2}}$ = 350 Hz) at

Table 1 Crystal data for $[IrRu_3(\eta^5\text{-}C_5Me_5)H(CO)_{10}BH_2]$ **4** and $[RhRu_3(\eta^5\text{-}C_5Me_5)H_2(CO)_8(PPh_3)BH]$ **5**[a]

Complex	4	5
(*a*) Crystal parameters		
Formula	$C_{20}H_{18}BIrO_{10}Ru_3$	$C_{36}H_{33}BO_8PRhRu_3$
Formula weight	924.6	1041.5
Crystal system	Triclinic	Monoclinic
Space group	$P\bar{1}$	$P2_1/n$
a/Å	8.780(1)	11.538(1)
b/Å	12.304(3)	18.141(2)
c/Å	12.432(3)	19.089(3)
α/°	105.78(2)	—
β/°	93.55(2)	102.98(1)
γ/°	91.44(2)	—
U/Å^3	1288.8(6)	3893.4(9)
Z	2	4
Crystal dimensions/mm	0.04 × 0.34 × 0.36	0.24 × 0.32 × 0.48
Colour	Orange	Dark red
D_c/g cm^{-3}	2.383	1.777
μ(Mo-Kα)/cm^{-1}	69.21	16.46
T/K	293	296
Transmission(min., max.)	0.345, 0.899	0.577, 0.755
(*b*) Data collection		
Data collected (h,k,l)	±11, ±15, ±16	±14, ±23, ±24
Reflections collected	6194	9482
Independent reflections	5919	8925
R_{merg}	1.46	2.46
Independent observed reflections $[F_o \geqslant n\sigma(F_o)]$	4601 (n = 5)	6347 (n = 4)
Variation in standards	<0.01	≈0.01
(*c*) Refinement		
R^b	0.0483	0.0368
R'^c	0.0623	0.0393
Δ/σ(max.)	0.06	0.003
$\Delta\rho$/e Å^{-3}	2.64	0.47
N_o/N_v	14.0	14.0
Goodness of fit^d	1.24	1.04
Weighting scheme	$w^{-1} = \sigma^2(F) + 0.0015F^2$	$w^{-1} = \sigma^2(F) + 0.0004F^2$

[a] Details in common: Siemens P3 diffractometer; graphite-monochromated Mo-Kα radiation (λ = 0.710 73 Å); scan range $4 < 2\theta < 55°$; three standard reflections every 197. [b] $R = \Sigma|F_o - F_c|/\Sigma F_o$. [c] $R' = \Sigma[|F_o - F_c|w^{\frac{1}{2}}]/\Sigma[F_o w^{\frac{1}{2}}]$. [d] Goodness of fit $= [\Sigma w|F_o - F_c|^2/(N_o - N_v)]^{\frac{1}{2}}$ where N_o is the number of observations and N_v the number of variables.

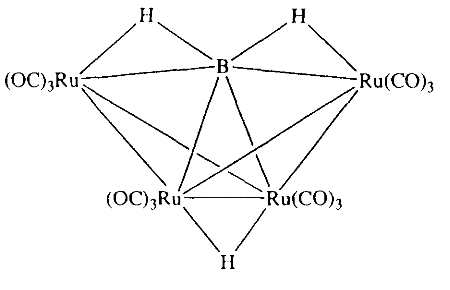

$[Ru_4H(CO)_{12}BH_2]$

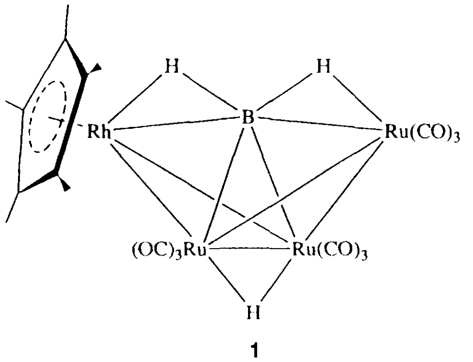

1

δ +94 ($CDCl_3$), somewhat shifted from the resonance for $[Ru_4H(CO)_{12}BH_2]$ (δ +109.9 in $CDCl_3$).[4] (The ^{11}B NMR spectral shift for $[Ru_4H(CO)_{12}BH_2]$, as for other clusters of this type, is solvent dependent[3,4]). The introduction of a heterometal atom is expected to influence the chemical shift of the boron atom and indeed, in the series $[Ru_4H(CO)_{12}BH_2]$, $[Ru_3FeH(CO)_{12}BH_2]$ and $[Fe_4H(CO)_{12}BH_2]$ a progressive movement of the ^{11}B NMR signal to lower field is observed.[1-4,6]

The ^1H NMR spectrum of **1** exhibits a signal due to the methyl protons of the η^5-C_5Me_5 ligand at δ +2.07. The mid- to high-field region of the spectrum shows a broad resonance at δ −9.6 and a sharp signal at δ −20.29. The latter resonance is typical of one arising from a Ru–H–Ru bridging hydride bonded along the Ru–Ru hinge edge of the tetrametal butterfly core; the hydride resonance is extremely sensitive to the exact environment of the cluster hydrogen atom with respect to the metal framework.[6,20,21] The close agreement between the values for the resonance assigned to the metal hydride in **1** and $[Ru_4H(CO)_{12}BH_2]$[3,4] provides evidence that the rhodium atom is located in a wing-tip rather than a hinge site. The resonance at δ −9.6 ($w_{\frac{1}{2}}$ = 300 Hz) is assigned to M–H–B (M = Ru or Rh) bridging hydrogen atoms. It was not possible to resolve this broad signal into components due to the separate Rh–H–B and Ru–H–B hydrogen atoms.

We were not able to grow single crystals of **1** but have confirmed the presence of the butterfly core *via* the full characterisation of the triphenylphosphine derivative, $[RhRu_3(\eta^5\text{-}C_5Me_5)H_2(CO)_8(PPh_3)BH]$ **5** which is described later in this paper.

Table 2 Atomic coordinates ($\times 10^4$) for $[IrRu_3(\eta^5\text{-}C_5Me_5)H(CO)_{10}BH_2]$ **4**

Atom	*x*	*y*	*z*
Ir	2 351(1)	3 758(1)	7 054(1)
Ru(1)	1 022(1)	1 572(1)	6 860(1)
Ru(2)	3 089(1)	1 258(1)	8 576(1)
Ru(3)	410(1)	2 331(1)	9 219(1)
B	2 365(12)	2 872(9)	8 225(9)
O(1)	−514(10)	4 824(7)	7 896(8)
O(2)	−820(11)	2 412(8)	5 086(7)
O(3)	−875(11)	−617(7)	6 565(7)
O(4)	3 292(12)	269(8)	5 323(8)
O(5)	4 724(12)	1 402(8)	10 847(8)
O(6)	5 794(13)	217(10)	7 292(10)
O(7)	1 647(11)	−1 082(7)	8 299(8)
O(8)	1 609(12)	2 620(8)	11 641(7)
O(9)	−2 162(12)	3 964(10)	9 871(8)
O(10)	−1 478(11)	186(8)	9 145(8)
C(1)	579(13)	4 383(9)	7 557(9)
C(2)	−116(14)	2 148(9)	5 776(9)
C(3)	−143(12)	183(9)	6 666(9)
C(4)	2 488(12)	804(9)	5 908(9)
C(5)	4 087(13)	1 372(8)	10 011(9)
C(6)	4 812(14)	639(10)	7 746(10)
C(7)	2 161(12)	−202(8)	8 422(9)
C(8)	1 194(12)	2 530(8)	10 721(10)
C(9)	−1 220(13)	3 358(10)	9 599(9)
C(10)	−758(12)	980(9)	9 204(9)
C(11)	4 527(12)	4 761(9)	7 313(10)
C(12)	4 809(12)	3 678(9)	6 619(10)
C(13)	3 914(14)	3 532(10)	5 559(10)
C(14)	3 098(14)	4 512(11)	5 622(10)
C(15)	3 444(12)	5 267(9)	6 715(10)
C(16)	5 357(16)	5 329(12)	8 412(12)
C(17)	6 002(15)	2 921(12)	6 841(14)
C(18)	3 984(19)	2 562(12)	4 512(12)
C(19)	2 105(18)	4 744(15)	4 665(13)
C(20)	2 856(17)	6 432(10)	7 113(14)

The second boron-containing product, **2**, in the reaction of either $[Ru_3(CO)_9BH_4]^-$ or $[Ru_3(CO)_9(B_2H_5)]^-$ with $[\{Rh(\eta^5\text{-}C_5Me_5)Cl_2\}_2]$ has been characterised by mass spectrometry and NMR and infrared spectroscopies. The parent envelope in the FAB mass spectrum of **2** is consistent with a formulation of $[RhRu_4(\eta^5\text{-}C_5Me_5)(CO)_{12}BH_3]$; the calculated isotopic distribution is in good agreement with that observed experimentally. The ^1H NMR spectrum exhibits a singlet at δ 1.98 which may be assigned to the $\eta^5\text{-}C_5Me_5$ ligand; this is consistent with the presence of an $\{Rh(\eta^5\text{-}C_5Me_5)\}$ unit. In the mid- to high-field part of the ^1H NMR spectrum, broad signals at δ −8.9 and −10.2 and a sharp resonance at δ −20.58 are characteristic of an asymmetrical tetrametal boron-containing butterfly structure and this geometry is further supported by a triplet (J_{BH} = 75 Hz) in the ^{11}B NMR spectrum at δ +101.6.[20] The infrared spectrum in the carbonyl region is instructive in that it reveals the presence of both terminal and bridging carbonyl ligands.

On the basis of the above data, we propose that compound **2** is the 76-electron cluster $[RhRu_4(\eta^5\text{-}C_5Me_5)H(CO)_{12}BH_2]$. The cluster core-geometries, **A** and **B**, shown in Fig. 1 are consistent with the 76-electron count; both are derived from the 74-electron square-based pyramid by breaking one of two different edges. Structure **A** has recently been confirmed for the boride $[Os_5H(CO)_{16}B]$.[5] However, on the basis that the ^1H NMR spectrum of **2** indicates the presence of two $M_{wing\text{-}tip}$–B bridging hydrogen atoms, core-structure **A** for **2** seems to be an unlikely choice for steric reasons. Structure **B** is a plausible geometry for **2**; it is reasonable that the presence of an edge-bridging $\{Ru(CO)_4\}$ unit will cause a rearrangement of the carbonyl ligands of the butterfly cluster core and result in the formation of at least one bridging carbonyl ligand as indicated in Fig. 1. It is of course possible that the boron atom resides within an Ru_4 framework and that the rhodium fragment is the remote unit. Confirmation of the structure must await an X-ray crystallographic study.

Reactions of Triruthenaborane Anions with $[\{Ir(\eta^5\text{-}C_5Me_5)Cl_2\}_2]$.—In contrast to the reaction of $[N(PPh_3)_2][Ru_3(CO)_9BH_4]$ with $[\{Rh(\eta^5\text{-}C_5Me_5)Cl_2\}_2]$, the reaction with $[\{Ir(\eta^5\text{-}C_5Me_5)Cl_2\}_2]$ leads to $[IrRu_3(\eta^5\text{-}C_5Me_5)H(CO)_{10}BH_2]$ **4** which possesses one more carbonyl ligand than the analogous rhodium product. A second pathway

Table 3 Atomic coordinates ($\times 10^4$) for $[RhRu_3(\eta^5\text{-}C_5Me_5)H_2(CO)_8(PPh_3)BH]$ **5**

Atom	*x*	*y*	*z*
Rh	2866.9(3)	6233.0(2)	1557.7(2)
Ru(1)	2991.5(3)	5611.0(2)	2872.7(2)
Ru(2)	357.3(3)	5802.3(2)	2672.8(2)
Ru(3)	1357.4(3)	5027.7(2)	1629.6(2)
P	−90(1)	6577.4(7)	3567.4(7)
O(1)	−2046(4)	5896(4)	1636(3)
O(2)	−220(5)	4382(3)	3355(3)
O(3)	4022(5)	6956(3)	3700(3)
O(4)	4297(4)	4522(3)	3997(2)
O(5)	5120(3)	5450(2)	2176(2)
O(6)	3038(4)	4417(3)	746(3)
O(7)	−523(4)	5659(2)	402(2)
O(8)	−34(4)	3619(3)	1771(3)
C(1)	−1157(5)	5864(4)	2035(3)
C(2)	−18(5)	4909(3)	3095(3)
C(3)	3633(5)	6442(3)	3394(3)
C(4)	3788(5)	4923(3)	3587(3)
C(5)	4163(5)	5629(3)	2217(3)
C(6)	2418(5)	4655(3)	1070(3)
C(7)	191(5)	5409(3)	855(3)
C(8)	500(5)	4140(3)	1739(3)
C(11)	3042(5)	7424(3)	1332(3)
C(12)	2187(5)	7123(3)	759(3)
C(13)	2753(5)	6561(3)	410(3)
C(14)	3976(5)	6552(3)	751(3)
C(15)	4155(5)	7060(3)	1337(3)
C(16)	2859(6)	8033(3)	1819(4)
C(17)	923(6)	7377(4)	504(4)
C(18)	2183(7)	6154(5)	−260(3)
C(19)	4913(6)	6063(4)	547(4)
C(20)	5332(5)	7254(4)	1813(4)
C(21)	184(6)	7915(3)	2905(3)
C(22)	−161(7)	8591(4)	2613(4)
C(23)	−1295(7)	8835(4)	2574(4)
C(24)	−2076(6)	8419(4)	2856(4)
C(25)	−1720(5)	7752(3)	3173(3)
C(26)	−580(4)	7491(3)	3198(3)
C(31)	−2298(5)	5946(3)	3543(3)
C(32)	−3236(5)	5718(4)	3831(3)
C(33)	−3185(6)	5796(4)	4546(3)
C(34)	−2182(7)	6098(5)	4985(3)
C(35)	−1252(6)	6338(4)	4696(3)
C(36)	−1290(5)	6256(3)	3976(3)
C(41)	1706(6)	6173(4)	4728(3)
C(42)	2570(6)	6294(4)	5349(4)
C(43)	2869(6)	6995(5)	5584(4)
C(44)	2347(6)	7577(4)	5201(4)
C(45)	1446(6)	7471(3)	4581(3)
C(56)	1117(4)	6765(3)	4343(3)
B	1587(5)	6135(3)	2068(3)

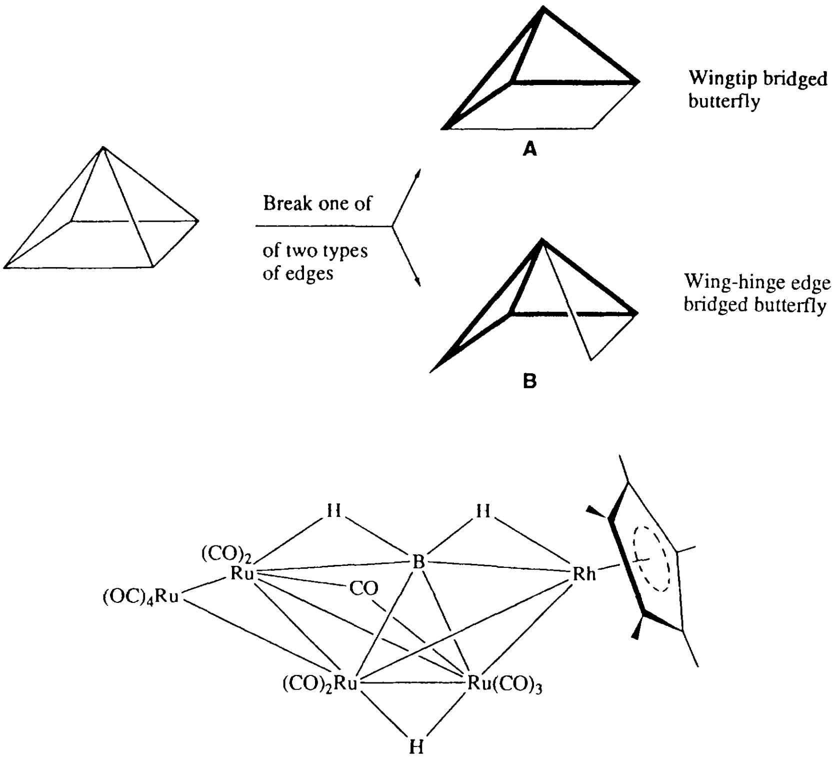

Fig. 1 Two possible geometries for the pentametal core of a 76-electron cluster, emphasising the incorporation of a butterfly unit; both are generated by breaking one edge of the square-based pyramid, and the proposed structure of [RhRu$_4$(η^5-C$_5$Me$_5$)H(CO)$_{12}$BH$_2$] **2**

exchanges the boron atom of the [Ru$_3$(CO)$_9$BH$_4$]$^-$ anion for an {Ir(η^5-C$_5$Me$_5$)} unit to give the neutral cluster [IrRu$_3$(η^5-C$_5$Me$_5$)H$_4$(CO)$_9$] **3**. This 60-electron cluster is proposed on the basis of spectroscopic data; the related tetrahedral clusters [IrOs$_3$(cp)H$_2$(CO)$_{10}$],[22] [RhOs$_3$(η^5-C$_5$Me$_5$)H$_4$(CO)$_9$][23] and [RhRu$_3$(η^5-C$_5$Me$_5$)H$_4$(CO)$_9$][16] have been structurally and spectroscopically characterised. The parent ion in the FAB mass spectrum of **3** shows an envelope at *m/z* 888, the isotopic pattern of which agrees with that simulated for [IrRu$_3$(η^5-C$_5$Me$_5$)H$_4$(CO)$_9$]. In the infrared spectrum, absorptions are consistent with the presence of terminal carbonyl ligands. The ^{1}H NMR spectrum exhibits a singlet at δ +2.20 assigned to the methyl groups of the η^5-C$_5$Me$_5$ ligand and a singlet at δ −18.71 at room temperature (CDCl$_3$) which remains sharp when the sample is cooled to 245 K (CD$_2$Cl$_2$). It is not possible to place four equivalent hydride ligands on the tetrahedral IrRu$_3$ core of **3** and thus the spectral data are interpreted in terms of a fluxional process that exchanges the four hydrogen atoms. Similarly, only one high-field ^{1}H NMR resonance is reported in solution at 293 K for [RhRu$_3$(η^5-C$_5$Me$_5$)H$_4$(CO)$_9$], although the crystal structure of this complex confirms the presence of two Ru–H–Ru and two Ru–H–Rh hydrogen environments in the solid state.[16] At 148 K (CD$_2$Cl$_2$–CFCl$_3$), the two cluster-hydrogen atom environments in [RhRu$_3$(η^5-C$_5$Me$_5$)H$_4$(CO)$_9$] are apparent in the ^{1}H NMR spectrum.[17] We propose that **3** has a similar structure to that of its rhodium congener, although we recognise that isomers with other arrangements of bridging hydrogen atoms are also possible.

When the starting cluster is [Ru$_3$(CO)$_9$(B$_2$H$_5$)]$^-$, the reaction with [{Ir(η^5-C$_5$Me$_5$)Cl$_2$}$_2$] yields **4** as the main product. The formulation of **4** as the 64-electron cluster [IrRu$_3$(η^5-C$_5$Me$_5$)H(CO)$_{10}$BH$_2$] was first suggested by mass and NMR spectroscopic data but the nature of the product was fully revealed by the results of an X-ray crystallographic study.

Molecular Structure of Compound **4**.—A crystal of **4**, suitable for X-ray analysis, was grown from CH$_2$Cl$_2$ layered with hexane. The molecular structure of **4** is shown in Fig. 2, and selected bond distances and angles are listed in Table 4. The boron atom lies within an open IrRu$_3$ skeleton which can be described as a spiked triangle or, within the context of this work, is recognised as an open butterfly framework. The boron atom is within bonding distance of all four metal atoms: Ir–B 2.04(1) Å and Ru–B 2.24(1), 2.25(1) and 2.36(1) Å. Three terminal carbonyl ligands are bonded to each ruthenium atom and the associated bond parameters are unexceptional. The iridium atom is present as an {Ir(η^5-C$_5$Me$_5$)(CO)} unit and obeys the eighteen electron rule if the Ir–Ru(1) and Ir–B interactions are considered to be localised. The relatively short Ir–B distance (compared to the Ru–B distances) is consistent with this premise. The three cluster hydrogen atoms were not located directly, but the solution ^{1}H NMR spectroscopic data, discussed below, are consistent with the presence of one M–H–M and two M–H–B bridging hydrogen atoms. A consideration of the orientations of the carbonyl ligands and cluster-core bond lengths leads us to propose that each of the edges Ru(2)–B, Ru(3)–B and Ru(1)–Ru(3) is bridged by a hydrogen atom.

The surprising feature of the structure of compound **4** is the presence of the carbonyl ligand on the iridium centre. Since the source of the Group 9 metal is a chloro dimer, the iridium-attached carbonyl must have arisen from adventitious CO, present in solution as a result of break-up of the triruthenium precursor. We observe that the yield of **4** can be significantly improved by passing a steady stream of carbon monoxide through the reaction solution. The extra carbonyl ligand provides the two electrons which boosts the cluster electron count from 62 to 64 and prevents the cluster framework from exhibiting the anticipated butterfly geometry. A schematic representation of the H$_3$IrRu$_3$B core of **4** is shown in Fig. 3 and is compared with the proposed butterfly-core structure of **1**. In preliminary work, we have made attempts to remove the tenth carbonyl ligand in **4** and induce a rearrangement to a 62-electron butterfly cluster analogous to **1** but, to date, these studies have not been successful.

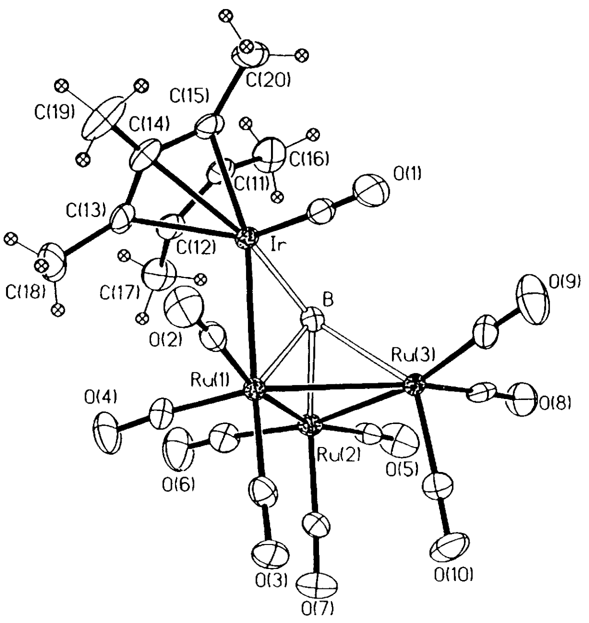

Fig. 2 Molecular structure of $[IrRu_3(\eta^5\text{-}C_5Me_5)H(CO)_{10}BH_2]$ **4**

Table 4 Selected bond lengths (Å) and angles (°) for $[IrRu_3(\eta^5\text{-}C_5Me_5)H(CO)_{10}BH_2]$ **4**

Ir–Ru(1)	2.847(1)	Ru(1)–Ru(2)	2.828(1)
Ru(1)–Ru(3)	2.914(1)	Ru(2)–Ru(3)	2.781(1)
Ir–B	2.04(1)	Ru(1)–B	2.238(9)
Ru(2)–B	2.25(1)	Ru(3)–B	2.36(1)
Ru(1)–Ir–B	51.3(3)	Ir–Ru(1)–Ru(2)	91.7(1)
Ir–Ru(1)–Ru(3)	88.7(1)	Ru(2)–Ru(1)–Ru(3)	57.9(1)
Ir–Ru(1)–B	45.4(3)	Ru(2)–Ru(1)–B	51.0(3)
Ru(3)–Ru(1)–B	52.5(3)	Ru(1)–Ru(2)–Ru(3)	62.6(1)
Ru(1)–Ru(2)–B	50.8(2)	Ru(3)–Ru(2)–B	54.7(3)
Ru(1)–Ru(3)–Ru(2)	59.5(1)	Ru(1)–Ru(3)–B	48.8(2)
Ru(2)–Ru(3)–B	51.0(3)	Ir–B–Ru(1)	83.3(4)
Ir–B–Ru(2)	143.5(5)	Ir–B–Ru(3)	132.2(5)
Ru(1)–B–Ru(2)	78.2(3)	Ru(1)–B–Ru(3)	78.6(3)
Ru(2)–B–Ru(3)	74.3(4)		

Solution Properties of Compound **4**.—In $CDCl_3$ solution, the room-temperature ^{11}B NMR spectrum of **4** exhibits two resonances of approximately equal intensity, and thus indicates the presence of two isomers. The shifts of δ +92.7 and +89.7 suggest that the environment of the boron atom in each isomer is similar. At room temperature, the ^1H NMR spectrum of **4** in CD_2Cl_2 exhibits two signals at δ +2.02 and +2.05 (1 : 1) assigned to two, similar $\eta^5\text{-}C_5Me_5$ environments, four broad resonances at δ −6.0, −6.4, −6.9 and −7.2 (approximately 1 : 1 : 1 : 1) assigned to Ru–H–B bridging hydrogen atoms and two sharp signals at δ −17.95 and −18.64 (1 : 1) assigned to two Ru–H–Ru bridging hydrogen atoms. The only significant change in the spectrum caused by lowering the temperature to 180 K is the sharpening of the broad signals due to thermal ^{11}B–^1H spin decoupling.[24,25] Over the range 298–330 K (in 1,1,2,2-$C_2D_2Cl_4$), the ^1H NMR spectra remain unchanged with the exception of increased broadening of the Ru–H–B resonances. Above 352 K, (in 1,1,2,2-$C_2D_2Cl_4$ solution), the two $\eta^5\text{-}C_5Me_5$ resonances begin to grow together; the two Ru–H–Ru resonances collapse and appear as one broad peak at 386 K, and the Ru–H–B resonances continue to broaden and, eventually, are seen as one very broad signal above 370 K. Spectral data were not collected above 386 K. These results are consistent with the onset of a dynamic process which interconverts the two isomers of **4**. Representative spectra are shown in Fig. 4. The ^{11}B and variable-temperature ^1H NMR spectroscopic data may be interpreted in terms of the process illustrated in Fig. 4 in which the $\{Ir(\eta^5\text{-}C_5Me_5)(CO)\}$ unit undergoes a localised site exchange. This may or may not be coupled with an exchange of the bridging hydride ligand between edges Ru(1)–Ru(2) and Ru(1)–Ru(3).

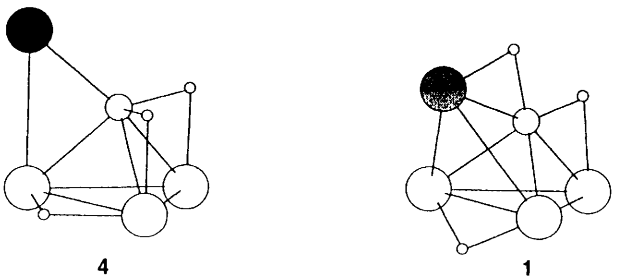

Fig. 3 Schematic representation of the open H_3IrRu_3B core of **4** with the butterfly core of **1** confirmed for the phosphine derivative **5**

Molecular Structure of Compound **5** *and Confirmation of the Cluster-core Geometry in* **1**.—As we were unable to grow X-ray quality crystals of **1**, we decided to prepare a simple phosphine substituted derivative. Compound **1** reacts readily with PPh_3 over a period of 1 h in CH_2Cl_2 to give a product **5**, for which mass spectral data are consistent with the replacement of one carbonyl ligand in **1** by a triphenylphosphine ligand; the ^{31}P NMR spectrum of **5** exhibits a single resonance at δ +35.5. However, the ^1H and ^{11}B NMR spectroscopic data for **5** are significantly different from those of **1**. The ^{11}B NMR spectral resonance for **5** is at δ +149 and this compares with δ +94 for **1**, thus indicating that **5** possesses a greater degree of direct metal-to-boron atom interaction[20,26,27] than does **1**. Consistent with this fact is the observation that the ^1H NMR spectrum of **5** exhibits signals due to one M–H–B and two M–H–M bridging interactions in contrast to the two M–H–B and one M–H–M interactions present in **1**.

A crystal of compound **5** of X-ray quality was grown from CH_2Cl_2 layered with hexane. The molecular structure is shown in Fig. 5 and selected bond distances and angles are listed in Table 5. The tetrametal framework of **5** possesses a butterfly geometry as expected with the $\{Rh(\eta^5\text{-}C_5Me_5)\}$ unit in one wing-tip site; this is consistent with the proposal for **1**. The boron atom is within bonding contact of all four metal atoms with distances Rh–B 1.952(6), Ru(1)–B 2.184(5), Ru(2)–B 2.108(6) and Ru(3)–B 2.169(5) Å. The internal dihedral angle of the butterfly framework is 109.7(1)°. The triphenylphosphine ligand occupies an equatorial site on the wing-tip ruthenium atom. Seven of the carbonyl ligands are terminally bound and are unexceptional. The carbonyl ligand C(5)O(5) is fully bridging between atoms Ru(1) and Rh; metal to carbon distances are Ru(1)–C(5) 2.039(6) and Rh–C(5) 2.043(5) Å. The appearance in the infrared spectrum of **5** (in CH_2Cl_2 solution) of an absorption at 1789 cm^{-1} is consistent with the presence of this bridging carbonyl ligand.

The three cluster hydrogen atoms have been located directly. One hydrogen atom bridges edge Ru(1)–Ru(3), the hinge of the butterfly skeleton. This is consistent with the observation of an ^1H NMR spectral resonance at δ −20.55. A second hydrogen atom bridges edge Ru(1)–Ru(2) and the hinge-wing-tip mode is characterised in the ^1H NMR spectrum by a signal at δ −14.41. The third cluster hydrogen atom is located in the site Ru(2)–H–B . The migration of one cluster hydrogen atom from an Rh–H–B site in **1** to a Ru_{wing}–H–Ru_{hinge} site in **5** corresponds to the change in the distribution of cluster electron density that accompanies the introduction of the phosphine ligand. Recently, we have reported a similar hydrogen redistribution in favour of metal- rather than boron-associated interactions in the series of clusters $[Ru_3(CO)_{9-x}(PPh_3)_xBH_5]$ $(3 \leqslant x \leqslant 0)$.[28]

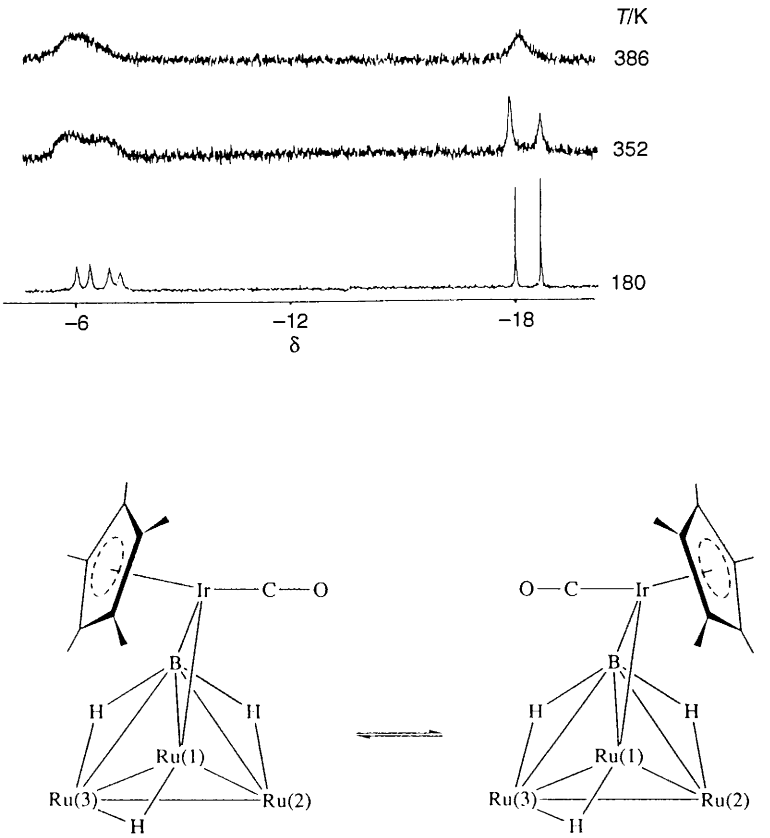

Fig. 4 Variable-temperature 400 MHz ^1H NMR spectra for compound **4** at 180 K (in $CDCl_3$) and 352 and 386 K (in 1,1,2,2-$C_2D_2Cl_4$) and a proposed process that will interconvert the two isomers of **4**

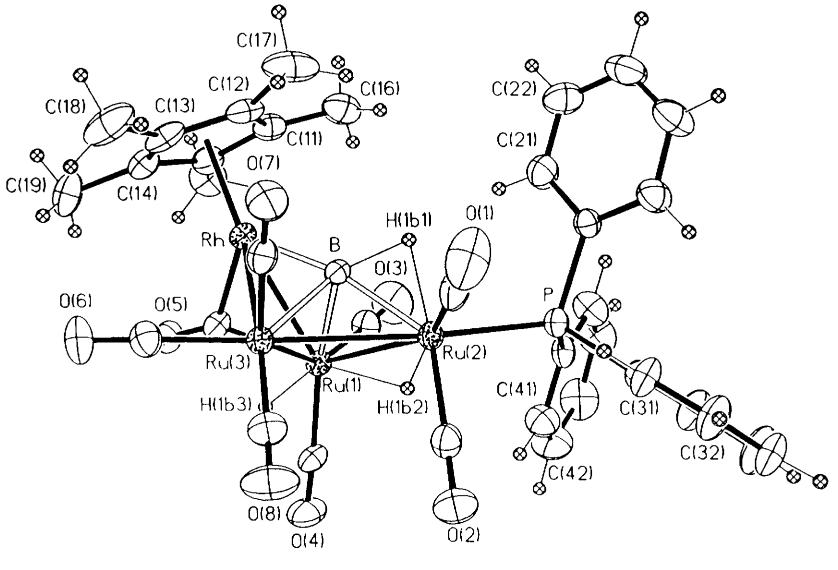

Fig. 5 Molecular structure of $[RhRu_3(\eta^5\text{-}C_5Me_5)H_2(CO)_8(PPh_3)BH]$ **5**

Conclusion

The study reported here illustrates differences in the reactivity of $[\{Rh(\eta^5\text{-}C_5Me_5)Cl_2\}_2]$ and $[\{Ir(\eta^5\text{-}C_5Me_5)Cl_2\}_2]$ with two triruthenaborane cluster anions. The boron-containing products $[RhRu_3(\eta^5\text{-}C_5Me_5)H(CO)_9BH_2]$ **1** and $[IrRu_3(\eta^5\text{-}C_5Me_5)H(CO)_{10}BH_2]$ **4** are related, but the incorporation of an extra carbonyl ligand in **4** means that the cluster core geometry of **4** is more open than that of **1**. Phosphine substitution in **1** not only provides an opportunity to confirm crystallographically the heterometallic core structure of **1** *via* that of the mono(triphenylphosphine) derivative but also illustrates once again the relationship between the site preference for cluster hydrogen atoms with charge distribution.[28]

Acknowledgements

We thank the donors of the Petroleum Research Fund, administered by the American Chemical Society for support of

Table 5 Selected bond lengths (Å) and angles (°) for $[RhRu_3(\eta^5\text{-}C_5Me_5)H_2(CO)_8(PPh_3)BH]$ **5**

Rh–Ru(1)	2.726(1)	Rh–Ru(3)	2.818(1)
Rh–B	1.952(6)	Ru(1)–Ru(2)	2.997(1)
Ru(1)–Ru(3)	2.880(1)	Ru(1)–B	2.184(5)
Ru(2)–Ru(3)	2.882(1)	Ru(2)–P	2.357(2)
Ru(2)–B	2.108(6)	Ru(3)–B	2.169(5)
Ru(1)–Ru–Ru(3)	62.6(1)	Ru(1)–Rh–B	52.5(1)
Ru(3)–Rh–B	50.2(2)	Rh–Ru(1)–Ru(2)	89.6(1)
Rh–Ru(1)–Ru(3)	60.3(1)	Ru(2)–Ru(1)–Ru(3)	58.7(1)
Rh–Ru(1)–B	45.2(2)	Ru(2)–Ru(1)–B	44.7(2)
Ru(3)–Ru(1)–B	48.4(1)	Ru(1)–Ru(2)–Ru(3)	58.6(1)
Ru(1)–Ru(2)–P	110.9(1)	Ru(3)–Ru(2)–P	168.1(1)
Ru(1)–Ru(2)–B	46.8(1)	Ru(3)–Ru(2)–B	48.6(1)
P–Ru(2)–B	120.6(1)	Rh–Ru(3)–Ru(1)	57.2(1)
Rh–Ru(3)–Ru(2)	90.2(1)	Ru(1)–Ru(3)–Ru(2)	62.7(1)
Rh–Ru(3)–B	43.7(2)	Ru(1)–Ru(3)–B	48.8(1)
Ru(2)–Ru(3)–B	46.8(2)	Rh–B–Ru(1)	82.3(2)
Rh–B–Ru(2)	167.8(3)	Rh–B–Ru(3)	86.1(2)
Ru(1)–B–Ru(2)	88.6(2)	Ru(1)–B–Ru(3)	82.9(2)
Ru(2)–B–Ru(3)	84.7(2)		

this work (grant No. 25533–AC3), the SERC for a studentship (to J. R. G.) and the National Science Foundation for a grant (CHE 9007852) towards the purchase of a diffractometer at the University of Delaware.

References

1 K. S. Wong, W. R. Scheidt and T. P. Fehlner, *J. Am. Chem. Soc.*, 1982, **104**, 1111.
2 T. P. Fehlner, C. E. Housecroft, W. R. Scheidt and K. S. Wong, *Organometallics*, 1983, **2**, 825.
3 F.-E. Hong, D. A. McCarthy, J. P. White, C. E. Cottrell and S. G. Shore, *Inorg. Chem.*, 1990, **29**, 2874.
4 A. K. Chipperfield, C. E. Housecroft and A. L. Rheingold, *Organometallics*, 1990, **9**, 681.
5 J. H. Chung, D. Knoeppel, D. A. McCarthy, A. Columbie and S. G. Shore, *Inorg. Chem.*, 1993, **32**, 3391.
6 S. M. Draper, C. E. Housecroft, A. K. Keep, D. M. Matthews, X. Song and A. L. Rheingold, *J. Organomet. Chem.*, 1992, **423**, 241.
7 C. E. Housecroft, D. M. Matthews, A. L. Rheingold and X. Song, *J. Chem. Soc., Dalton Trans.*, 1992, 2855.
8 J. A. Hriljac, S. Harris and D. F. Shriver, *Inorg. Chem.*, 1988, **27**, 816.
9 J. A. Hriljac, P. N. Swepston and D. F. Shriver, *Organometallics*, 1985, **4**, 158.
10 J. W. Kolis, E. M. Holt, J. A. Hriljac and D. F. Shriver, *Organometallics*, 1984, **3**, 496.
11 E. M. Holt, J. A. Hriljac and D. F. Shriver, *Inorg. Chem.*, 1987, **26**, 2943.
12 M. P. Jensen, W. Henderson, D. H. Johnston, M. Sabat and D. F. Shriver, *J. Organomet. Chem.*, 1990, **394**, 121.
13 C. K. Schauer and D. F. Shriver, *Angew. Chem., Int. Ed., Engl.*, 1987, **26**, 255.
14 C. E. Housecroft, D. M. Matthews, A. Waller, A. J. Edwards and A. L. Rheingold, *J. Chem. Soc., Dalton Trans.*, 1993, 3059.
15 A. K. Chipperfield and C. E. Housecroft, *J. Organomet. Chem.*, 1988, **349**, C17.
16 W. E. Lindsell, C. B. Knobler and H. D. Kaesz, *J. Organomet. Chem.*, 1985, **296**, 209.
17 W. E. Lindsell, N. M. Walker and A. S. F. Boyd, *J. Chem. Soc., Dalton Trans.*, 1988, 675.
18 C. R. Eady, B. F. G. Johnson and J. Lewis, *J. Chem. Soc., Dalton Trans.*, 1977, 477.
19 G. Sheldrick, Siemens XRD, Madison, WI.
20 C. E. Housecroft, *Adv. Organomet. Chem.*, 1991, **33**, 1 and refs. therein.
21 M. L. Blohm, D. E. Fjare and W. L. Gladfelter, *J. Am. Chem. Soc.*, 1986, **108**, 2301.
22 L.-Y. Hsu, W.-L. Hsu, D. A. McCarthy, J. A. Krause, J.-H. Chung and S. G. Shore, *J. Organomet. Chem.*, 1992, **426**, 121.
23 D.-Y. Jan, L.-Y. Hsu, W.-L. Hsu and S. G. Shore, *Organometallics*, 1987, **6**, 274.
24 H. Beall and C. H. Bushweller, *Chem. Rev.*, 1973, **73**, 465.
25 C. H. Bushweller, H. Beall, M. Grace, W. J. Dewkett and H. S. Bilofsky, *J. Am. Chem. Soc.*, 1971, **93**, 2145.
26 N. P. Rath and T. P. Fehlner, *J. Am. Chem. Soc.*, 1988, **110**, 1111.
27 T. P. Fehlner, P. T. Czech and R. F. Fenske, *Inorg. Chem.*, 1990, **29**, 3103.
28 C. E. Housecroft, D. M. Matthews, A. J. Edwards and A. L. Rheingold, *J. Chem. Soc., Dalton Trans.*, 1993, 2727.

Received 25*th August* 1993; *Paper* 3/05146C